



Molecular emissions in sonoluminescence spectra of water sonicated under Ar-based gas mixtures

R. Pflieger, E. Fayard, C. Noël, Sergey I. Nikitenko, T. Belmonte

► To cite this version:

R. Pflieger, E. Fayard, C. Noël, Sergey I. Nikitenko, T. Belmonte. Molecular emissions in sonoluminescence spectra of water sonicated under Ar-based gas mixtures. *Ultrasonics Sonochemistry*, 2019, 58, pp.104637. <10.1016/j.ultsonch.2019.104637>. <hal-02425241>

HAL Id: hal-02425241

<https://hal.science/hal-02425241v1>

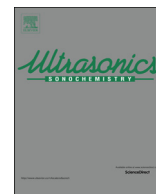
Submitted on 7 Sep 2020

HAL is a multi-disciplinary open access archive for the deposit and dissemination of scientific research documents, whether they are published or not. The documents may come from teaching and research institutions in France or abroad, or from public or private research centers.

L'archive ouverte pluridisciplinaire **HAL**, est destinée au dépôt et à la diffusion de documents scientifiques de niveau recherche, publiés ou non, émanant des établissements d'enseignement et de recherche français ou étrangers, des laboratoires publics ou privés.



HAL Authorization



Molecular emissions in sonoluminescence spectra of water sonicated under Ar-based gas mixtures

R. Pflieger^{a,*}, E. Fayard^a, C. Noel^b, S.I. Nikitenko^a, T. Belmonte^b

^a Institut de Chimie Séparative de Marcoule, ICSM UMR 5257 – CEA, CNRS, Univ Montpellier, ENSCM, Bagnols-sur-Cèze Cedex, France

^b Université de Lorraine, Institut Jean Lamour, UMR CNRS 7198, Nancy, France

ARTICLE INFO

Keywords:

Sonochemistry
Sonoluminescence
Emission spectra
Ultrasound
Plasma

ABSTRACT

Sonoluminescence (SL) spectroscopy is one of the very few ways to study the plasma formed in solutions submitted to ultrasound. Unfortunately, up to now only very limited emission bands were reported in SL spectra of aqueous solutions, moreover broad and badly resolved. It is shown here that by adding some N₂ and/or CO₂ in Ar, new molecular emissions (CN, N₂ and CO) can be observed and that for some of them rovibronic temperatures can be derived. The paramount importance of Stark broadening in these emissions is underlined, together with the need for data on Stark parameters for molecular emissions.

1. Introduction

When a liquid is irradiated by ultrasounds (US) emitted at a frequency set in the range 20 kHz–1 MHz, a particular chemical activity is observed, called sonochemistry. Its origin is acoustic cavitation: nucleation, growth and violent collapse of microbubbles containing dissolved gases and vapour of the bulk liquid. The formation of a plasma in cavitation bubbles at collapse is now widely admitted [1] even though the underlying mechanism remains unclear. Moreover characterization of this plasma is not straightforward due to its small size (< 1 μm), its short lifespan (< 1 ns) and the stochastic (non-predictable) nature of its apparition. Two main directions can be followed to study it: monitoring of its chemical activity and emission spectroscopy of its sonoluminescence (SL, the light emitted by the sonochemical plasma). Yet, and despite the obvious qualities of water as a solvent, relatively few atomic and molecular emissions have been reported in SL spectra of aqueous solutions and limited information about the plasma characteristics could be derived from them.

Reported molecular emissions are those from OH [2], C₂ [3] and NH [4] radicals and from non-volatile solutes such as alkali metals [5], lanthanide Ln(III) ions [6] and uranyl UO₂²⁺ ions [7]. Different excitation mechanisms do exist: excitation by the photons of sonoluminescence (sonophotoluminescence) of ions in solution (e.g. Ce³⁺ [8] or UO₂²⁺ [7]), collisional excitation at the bubble interface [7] or formation in the intra-bubble plasma [9]. The latter case being common, these emissions have been used to characterize the formed plasma or more generally the conditions reached at collapse.

For instance, emissions from alkali were the focus of various studies aiming at determining the maximum pressure reached in cavitation bubbles. The made assumption was that pressure (or more exactly the intra-bubble density) was the main parameter affecting the line shift and broadening of the emissions. Lepoint-Mullie et al. [5a] measured Rb resonance line shifts in sonoluminescence of RbCl aqueous solutions sonicated at 20 kHz under Ar or Kr, compared them with tabulated ones vs. relative density and deduced a relative density of 18 ± 2 . Similar results were obtained in silicon oil with the same approach [10]. On the other hand, relative densities derived from line broadening were much higher: 36–50 at 460 kHz under Ar [11], 59.5 at 138 kHz under Ar [12], corresponding to 885 bar if a temperature of 4300 K is considered or 800–1200 bar at 22 and 44 kHz under Ar [13]. The discrepancy in the values obtained with these two approaches was attributed to the non-negligible contribution of Stark effects in both broadening and shift [4b].

Rovibronic temperatures of excited species, obtained from simulation of the SL spectra, were also used to estimate the peak temperature reached at collapse. In early works, unicity of the temperature was assumed. Didenko et al. [3a] fitted C₂ Swan (d³Π_g – a³Π_u) bands in the SL spectra of an aqueous 10^{−3} M benzene solution sonicated at 20 kHz under Ar and obtained a temperature of 4300 ± 200 K. More recently, a study [3b] at different ultrasonic frequencies of Swan bands in SL spectra of aqueous *tert*-butanol solutions under Ar showed the necessity of considering the non-equality of the vibrational T_v and rotational T_r temperatures (T_v > T_r). Temperatures (± 1000 K) estimated in the *tert*-butanol concentration range where the intensity of Swan bands was

* Corresponding author.

E-mail address: rachel.pflieger@cea.fr (R. Pflieger).

<https://doi.org/10.1016/j.ultsonch.2019.104637>

Received 10 April 2019; Received in revised form 5 June 2019; Accepted 11 June 2019

Available online 11 June 2019

1350-4177/ © 2019 Elsevier B.V. All rights reserved.

highest were e.g. $T_v = 6300$ K and $T_r = 4800$ K at 20 kHz and $T_v = 8000$ K and $T_r = 4000$ K at 362 kHz. Similar temperatures and the same trend of an increase in vibrational temperatures at high US frequency were obtained from fits of OH ($A^2\Sigma^+ - X^2\Pi$) and NH ($A^3\Pi - X^3\Sigma^-$) emissions in SL spectra of 0.1 M ammonia solutions under Ar: for OH $T_v = 9000 \pm 1000$ K and $T_r = 5000 \pm 500$ K at 20 kHz, and $T_v = 13000 \pm 2000$ K and $T_r = 6000 \pm 1000$ K at 359 kHz, for NH $T_v = 7000 \pm 1000$ K and $T_r = 4000 \pm 500$ K at 20 kHz, and $T_v = 10000 \pm 1000$ K and $T_r = 2200 \pm 500$ K at 359 kHz.

The comparison of these values shows a large variation. Thus, the need for information on the plasma formed in cavitation bubbles remains essential and it is important to gain a better understanding of mechanisms controlling molecular emissions produced in known conditions and in systems as simple as possible. The present work focuses on high-frequency (362 kHz) SL spectra of water saturated with gas mixtures in Ar. The added gases and their concentrations were beforehand optimised to allow the observation of some new molecular emissions (CN, CO) in SL without decreasing much the SL intensity, and of already reported ones (OH, NH, C_2). Rovibronic temperatures and broadening parameter are determined and compared.

2. Experimental methods

For all experiments, 250 mL of deionized water (Milli-Q 18.2 M Ω cm) were placed in a thermostated glass reactor equipped with a 362-kHz transducer (ELAC Nautik, 25 cm²) at its bottom. The absorbed acoustic power was determined calorimetrically ($P_{ac} = 43$ W). The solution was submitted to a continuous gas flow (82 mL/min) of Ar or mixtures of N₂ (5%) and/or CO₂ (0.5%) in Ar (all gases with a purity > 99.999%, and provided by Air Liquide), starting half an hour before the experiment and maintained during the ultrasonic treatment.

Emission spectra of sonoluminescence were collected through a flat quartz window mounted on the sonoreactor and recorded in the spectral range 250–650 nm by means of SP 2356i Roper Scientific spectrometer (gratings 150blz500, 600blz300 and 1200blz300; 50 μ m slit) coupled with a CCD camera that is equipped with UV coating (SPEC10-100BR Roper Scientific) cooled by liquid nitrogen. Spectral calibration was performed using a Hg(Ar) pen-ray lamp (LSP035, LOT-Oriel). The spectra acquisition was started after reaching a steady-state temperature. For each experiment, at least ten 300-s (150blz500 grating), respectively 600-s (600blz300 and 1200blz300 gratings), spectra were averaged and corrected for the background noise and for the quantum efficiencies of gratings and CCD.

Molecular emissions were fitted using Specair [14] software after removal of a linear baseline. Computation parameters were the vibrational and rotational temperatures (T_v and T_r) of the considered species, the gas temperature, taken equal to T_r , and the pressure p . Instrumental broadening was taken into account by convoluting calculated spectra with an experimental slit function. Due to the relatively high signal scattering, the low spectral resolution and the strong broadening of the emissions, an automatic fitting was not possible and the computation parameters were fitted manually in a row to reproduce the relative intensities of the different rovibronic transitions (T_v , T_r) and the width of the peaks (p).

Gases formed during the sonolysis were measured online by mass spectrometry (Prima BT, Thermo Fischer Scientific). Monitored masses are given in Table 1. The fragment N ($m/z = 14$) was recorded to discriminate CO from N₂ ($m/z = 28$). MS analysis was started at the same time as pre-saturation of the solution, i.e. at least half an hour before the beginning of sonication, to record a baseline for each monitored species. In the particular case of CO, this baseline includes the ion intensities of N₂ and of the fragment CO of CO₂. The increase in ion intensity of $m/z = 28$ during the sonolysis is due to CO gas and comparison of the ion intensities during sonolysis and of the baseline allows to quantify its amount.

Table 1

Masses (amu) of the gases monitored by mass spectrometry.

m/z , amu	Species
40	Ar
2	H ₂
28	N ₂ and/or CO
32	O ₂
44	CO ₂
14	N

Table 2

Chemical yields of the formed gaseous products, H₂ and CO.

Saturating gas	H ₂ yield, μ mol/kJ (± 0.02)	CO yield, μ mol/kJ (± 0.6)
Ar	0.36	–
Ar-5%N ₂	0.27	–
Ar-0.5%CO ₂	0.09	1.7
Ar-0.5%CO ₂ -5%N ₂	0.12	–

3. Results & discussion

3.1. Formed gaseous products

Table 2 summarizes the chemical yields of the observed gaseous products of the sonolysis for the various gas mixtures. Hydrogen arises from the dissociation of water molecules in cavitation bubbles at collapse and subsequent recombination of radicals (where))) stands for a reaction induced by ultrasound):



As soon as some amount of molecular gas is added in Ar, the H₂ yield decreases. This effect can be partly attributed to the less efficient energy concentration at collapse [15] and the additional losses in energy due to higher thermal conductivity of molecules, vibrational and rotational excitations and chemical reactions, translating into a less energetic plasma, but also to additional reactions consuming H radicals and/or H₂ molecules. It is known [4a,16] that the following reactions involving nitrogen and hydrogen take place in cavitation bubbles during the high-frequency sonolysis of water saturated with Ar-N₂, leading to a decrease in H₂ formation yield:



The reduction in H₂ yield in the presence of CO₂ may be attributed to the reactions of CO₂ with H atoms [17]:



The subsequent reaction of this latter radical with H atoms leads to the formation of formic acid, as previously reported by Henglein [17b] who showed that the main product of the 300-kHz sonolysis of water presaturated with Ar-CO₂ mixtures was carbon monoxide, with some amount of formic acid. Reaction (8) would also explain the observed formation of CO in the sonolysis of water saturated with Ar-0.5%CO₂ and the concomitant similar decrease in CO₂ ion intensity (of $1.4 \pm 0.6 \mu$ mol/kJ). A second reaction can also lead to CO formation

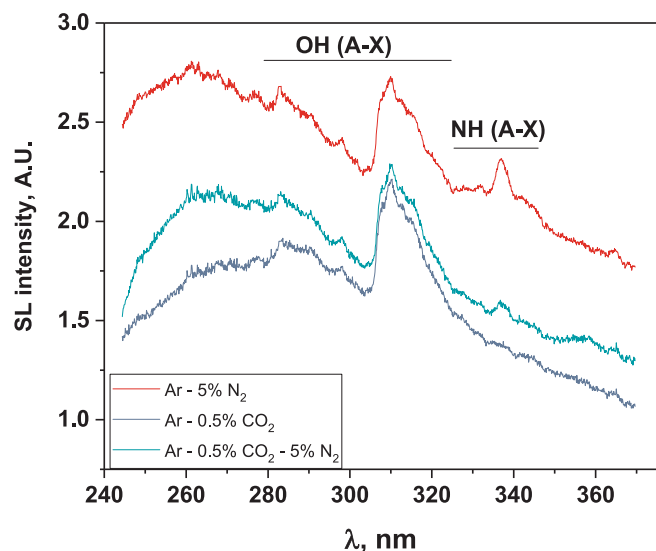
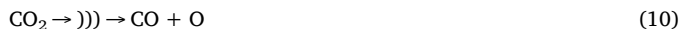
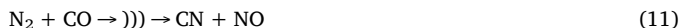


Fig. 1. UV part of SL spectra of water under Ar-5%N₂, Ar-0.5%CO₂ and Ar-0.5%CO₂-5%N₂ (362 kHz, 43 W, 14 °C, 600blz300 grating).

[17b]:



Adding conjointly 0.5% CO₂ and 5% N₂ in Ar leads to the disappearance of CO in the outlet gas, which can be traced back to the reaction [17a] of CO with N₂:



Reaction (11) would also account for the lesser decrease in H₂ yield with this ternary gas mixture compared to the binary ones Ar-5%N₂ and Ar-0.5%CO₂, less CO₂ and N₂ molecules being available for quenching H atoms.

3.2. Observed molecular emissions in sonoluminescence emission spectra

Fig. 1 presents the UV parts of SL spectra of water sonicated at 362 kHz under Ar-5%N₂, Ar-0.5%CO₂ and Ar-0.5%CO₂-5%N₂ gas flows, and Fig. 2 their visible parts.

Like the usually reported SL spectra of water under Ar, they show an

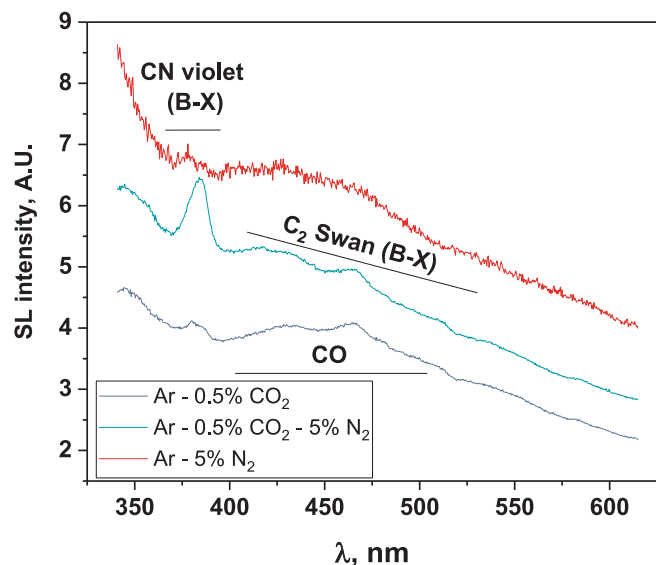
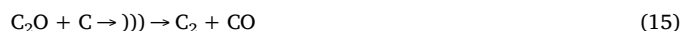


Fig. 2. Visible part of SL spectra of water under Ar-5%N₂, Ar-0.5%CO₂ and Ar-0.5%CO₂-5%N₂ (362 kHz, 43 W, 14 °C, 150blz500 grating).

intense continuum spanning from the UV to the near IR and the emission from excited OH radicals (OH (A-X)). The latter arise from the dissociation of water molecules in cavitation bubbles at collapse (reaction (1)). When the saturating gas is Ar-5%N₂, a molecular emission is present around 337 nm that is assigned to NH (A-X) [4a]. A probable mechanism of formation of this excited species is given by reactions (5)–(7).

The sonolysis of water in the presence of Ar-0.5%CO₂ gas mixture leads to a complex SL spectrum. A tiny peak appears near 386 nm and is attributed to CN violet [18]; indeed, CN can be formed in the presence of air traces by reaction (11) [17a].

Besides, the maxima of C₂ Swan bands are recognizable but superimpose with a broad not-well-defined emission, or a sum of emissions, likely from CO (possibly CO (X-X) [18] (Fig. 1SI), CO (C-A) and CO (d-a) [18]). This hypothesis on the nature of this emission is supported by the presence of CO in the outlet gas (Table 2). The ultrasonically driven formation of C₂ excited species in the presence of CO gas was recently [19] reported and explained by CO disproportionation followed by the recombination of carbon atoms and/or formation and subsequent dissociation of C₂O molecules [20]:



Adding conjointly 0.5% CO₂ and 5% N₂ in Ar leads to the observation of OH (A-X), NH (A-X), CN violet (confirming the nature of the emission at 386 nm) and C₂ Swan bands. In this gas mixture, CN formation can also be attributed to following reaction [21]:



The absence of CO emission in the SL spectra of water saturated with Ar-0.5%CO₂-5%N₂ correlates with the absence of CO in the outlet gas (Table 2).

3.3. Derived rovibronic temperatures

Fig. 3 compares the OH (A-X) emissions observed with the different gas mixtures in Ar (after subtraction of a baseline due to the SL continuum). They are very similar, except for two zones (indicated by arrows) where the intensity is higher when N₂ is present in the gas:

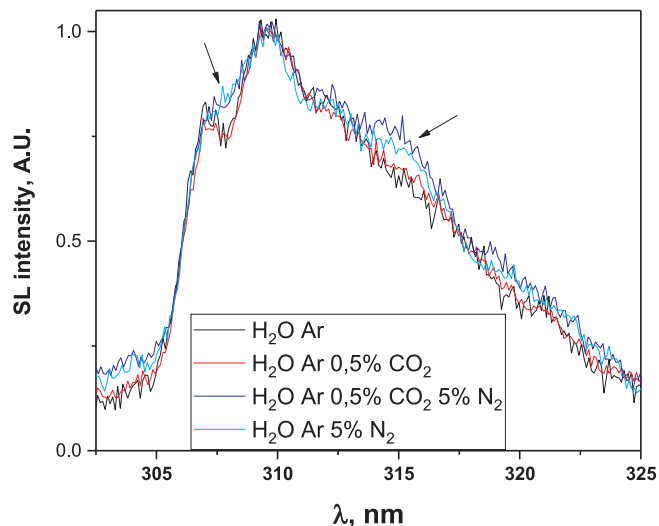


Fig. 3. Comparison of OH emission in SL spectra of water sparged with gas mixtures in Ar.

Table 3Estimated rovibronic temperatures (± 1000 K unless otherwise specified) and effective pressures (± 300 bar) by simulations with Specair software.

Gas	OH	NH	C ₂	CN
Ar	9000 K/6500 K/1000 bar			
Ar – 5% N ₂		10000 K/10000 K/4000 bar		
Ar – 0.5% CO ₂				
Ar – 0.5% CO ₂ – 5% N ₂			22000 K/5000 K/6000 bar	10000–15000 K/10000 K/10000 bar

around 308 nm and around 315 nm. The former may be due to NH (c-a) and/or to N₂ (C-B) and the latter to N₂ (C-B) emissions (Fig. 2SI in Supporting Information), superimposed on that of OH. Thus simulation was performed (using Specair software [14]) on OH (A-X) emission under Ar (Fig. 3SI in Supporting Information). It can be reasonably fitted with $T_v = 9000$ K (± 1000 K), $T_r = 6500$ K (± 1000 K) and an effective pressure of 1000 bar (± 300 bar).

The simulation of NH (A-X) in the presence of Ar-5%N₂ (Fig. 4SI in Supporting Information) leads to $T_v = 10000$ K (± 1000 K), $T_r = 10000$ K (± 1000 K) and an effective pressure of 4000 bar (± 500 bar). The bulge around 340–345 nm is of unknown origin. Interestingly, when N₂ content in Ar is increased, NH (A-X) emission cannot be fitted anymore, which is attributed to the presence of a non-negligible N₂ (C-B) emission (Fig. 2SI in Supporting Information).

Due to the presence of a strong CO emission in the SL spectra of water saturated with Ar-0.5%CO₂, the simulation of C₂ Swan bands could be performed only for the gas mixture Ar-5%N₂-0.5%CO₂ for which no CO emission was noted. It was done focusing on the $\Delta\nu = 0$ and $\Delta\nu = 1$ bands (Fig. 5SI in Supporting Information). Derived rovibronic temperatures are $T_v = 22000$ K (± 1000 K), $T_r = 5000$ K (± 1000 K) and an effective pressure of 6000 bar (± 1000 bar).

In the presence of the gas mixture Ar-5%N₂-0.5%CO₂ an intense CN (B-X) molecular emission is also observed that can be simulated with $T_v = 12500$ K (± 2500 K), $T_r = 10000$ K (± 1000 K) and an effective pressure of the order of 10000 bar (Fig. 6SI in Supporting Information).

Table 3 summarizes all derived rovibronic temperatures and effective pressures in the form vibrational temperature T_v /rotational temperature T_r /effective pressure.

The very large effective pressure values obtained, in particular from CN emission, and the fact that they considerably differ depending on which emitting species is considered, undoubtedly confirm that pressure cannot be considered as the main broadening parameter, as previously discussed [4b] and that Stark broadening should be taken into account. Unfortunately however, data on Stark broadening of molecular emissions are particularly scarce, which considerably limits the information that can be derived from the measured broadenings.

Comparison of the present OH rovibronic temperatures with previously [2d] reported ones for the sonication of water at 362 kHz under Ar shows a good agreement for both T_v (9000 vs. 8000 K) and T_r (6500 vs. 5250 K), whereby the difference may be due to the uncertainty in the baseline definition. Similarly, a difference in the continuum shape in the wavelength range of OH emission may also account for the higher T_v reported for OH in a 0.1 M ammonia solution [4b] (13000 K).

In the presence of Ar – 5% N₂ two molecular emissions are observed, the vibrational temperatures of which are fairly close, while NH rotational temperature is higher than that of OH. Interestingly, it is also much higher than the rotational temperature derived from NH emission in the sonolysis of an ammonia solution [4b] (2200 K). Considering the different reaction pathways leading to NH formation in both cases (sonolysis of NH₃ molecule vs. reactions (1) & (5)–(7)) it is conceivable that the formation of NH from H and N radicals necessitates several steps compared to the direct sonolysis of NH₃ or H₂O molecules. Then, the chemical pathway leading to emission likely affects the rotational distribution of the emitting states, leading to the observed discrepancy between measurements.

A similar disagreement is observed between the derived rovibronic

temperatures for the gas mixture Ar – 0.5% CO₂ – 5% N₂. The several steps leading to CN formation may also lead to specific rotational populations and rotational temperature that do not match with the gas temperature, due to the extremely short lifetime of the formed plasma. For the same reason, vibrational temperatures might be different as well.

4. Conclusion

Although it was long considered that SL spectra of aqueous solutions were relatively featureless compared to those of exotic liquids (e.g. concentrated sulfuric acid), thus strongly limiting the possibility to study the formed plasma, this study shows that besides usual OH and C₂ emissions and the recently reported NH one, at least three more molecular emissions can be observed in high-frequency SL spectra of aqueous solutions, namely CN, N₂ and CO. This finding enriches the “toolbox” available to characterize the sonochemical plasma, the conditions reached at collapse of cavitation bubbles and the chemical reactions taking place in bubble cores.

Unfortunately, not all these emissions can be fitted yet: CO blends into the continuum and N₂ superimposes over the strong OH emission. Moreover, their presence perturbs the fitting of the other better-defined emissions, like C₂ or OH.

To go further in the exploitation of these emissions, there is a strong need for tabulated data on Stark parameters for molecular emissions. Once available, the present data might allow estimation of the reached pressure and of plasma characteristics such as electron density and temperature. The optimised three-component gas mixture is in this purpose of particular interest since the corresponding SL spectra present three different usable molecular emissions.

Acknowledgements

CNRS and in particular its Réseau des Plasmas Froids are acknowledged for supporting this work with an IPMC.

Appendix A. Supplementary data

Supplementary data to this article can be found online at <https://doi.org/10.1016/j.ultsonch.2019.104637>.

References

- [1] P.J. Bruggeman, M.J. Kushner, B.R. Locke, J.G.E. Gardeniers, W.G. Graham, D.B. Graves, R. Hofman-Caris, D. Maric, J.P. Reid, E. Ceriani, D.F. Rivas, J.E. Foster, S.C. Garrick, Y. Gorbanev, S. Hamaguchi, F. Iza, H. Jablonowski, E. Klimova, J. Kolb, F. Krema, P. Lukes, Z. Machala, I. Marinov, D. Mariotti, S.M. Thagard, D. Minakata, E.C. Neyts, J. Pawlat, Z.L. Petrovic, R. Pflieger, S. Reuter, D.C. Schram, S. Schroter, M. Shiraiwa, B. Tarabova, P.A. Tsai, J.R.R. Verlet, T. von Woedtke, K.R. Wilson, K. Yasui, G. Zvereva, *Plasma Sources Sci. Technol.* 25 (5) (2016) 053002.
- [2] (a) C. Sehgal, R.G. Sutherland, R.E. Verrall, *J. Phys. Chem.* 84 (4) (1980) 388–395; (b) T.V. Gordeychuk, Y.T. Didenko, S.P. Pugach, *Acoust. Phys.* 42 (2) (1996) 240–241; (c) T. Lepoint, F. Lepoint-Mullie, N. Voglet, S. Labouret, C. Petrier, R. Avni, J. Luque, *Ultrason. Sonochem.* 10 (3) (2003) 167–174; (d) R. Ji, R. Pflieger, M. Viot, S.I. Nikitenko, *J. Phys. Chem. B* 122 (27) (2018) 6989–6994.
- [3] (a) Y.T. Didenko, W.B. McNamara, K.S. Suslick, *J. Am. Chem. Soc.* 121 (24) (1999) 5817–5818;

- (b) R. Pflieger, A.A. Ndiaye, T. Chave, S.I. Nikitenko, J. Phys. Chem. B 119 (1) (2015) 284–290.
- [4] (a) T. Ouerhani, R. Pflieger, W. Ben Messaoud, S.I. Nikitenko, J. Phys. Chem. B 119 (2015) 15885–15891;
(b) R. Pflieger, T. Ouerhani, T. Belmonte, S.I. Nikitenko, PCCP 19 (38) (2017) 26272–26279.
- [5] (a) F. Lepoint-Mullie, N. Voglet, T. Lepoint, R. Avni, Ultrason. Sonochem. 8 (2) (2001) 151–158;
(b) S. Abe, P.K. Choi, Jpn. J. Appl. Phys. 48 (2009) 7;
(c) C. Cairos, J. Schneider, R. Pflieger, R. Mettin, Ultrason. Sonochem. 21 (6) (2014) 2044–2051;
(d) G.L. Sharipov, B.M. Gareev, A.M. Abdrakhmanov, Acoust. Phys. 59 (5) (2013) 521–527.
- [6] (a) G.L. Sharipov, JETP Lett. 85 (9) (2007) 458–460;
(b) G.L. Sharipov, R.K. Gainetdinov, A.M. Abdrakhmanov, Russ. Chem. Bull. 52 (9) (2003) 1969–1973;
(c) G.L. Sharipov, B.M. Gareev, A.M. Abdrakhmanov, JETP Lett. 91 (11) (2010) 566–569;
(d) R. Pflieger, J. Schneider, B. Siboulet, H. Mohwald, S.I. Nikitenko, J. Phys. Chem. B 117 (10) (2013) 2979–2984.
- [7] R. Pflieger, V. Cousin, N. Barre, P. Moisy, S.I. Nikitenko, Chem.-Eur. J. 18 (2) (2012) 410–414.
- [8] G.L. Sharipov, R.K. Gainetdinov, A.M. Abdrakhmanov, Russ. Chem. Bull. 57 (9) (2008) 1831–1836.
- [9] (a) G.L. Sharipov, A.M. Abdrakhmanov, B.M. Gareev, Tech. Phys. 58 (2) (2013) 255–258;
(b) C. Cairos, R. Mettin, Phys. Rev. Lett. 118 (2017) 6.
- [10] W.B. McNamara, Y.T. Didenko, K.S. Suslick, Nature 401 (6755) (1999) 772–775.
- [11] C. Sehgal, R.P. Steer, R.G. Sutherland, R.E. Verrall, J. Chem. Phys. 70 (5) (1979) 2242–2248.
- [12] P.K. Choi, S. Abe, Y. Hayashi, J. Phys. Chem. B 112 (3) (2008) 918–922.
- [13] M.V. Kazachek, T.V. Gordeychuk, Tech. Phys. Lett. 35 (2) (2009) 193–196.
- [14] C.O. Laux, T.G. Spence, C.H. Kruger, R.N. Zare, Plasma Sources Sci. Technol. 12 (2) (2003) 125–138.
- [15] F.R. Young, Sonoluminescence, CRC Press, New York, 2005.
- [16] Supeno, P. Kruus, Ultrason. Sonochem. 9 (1) (2002) 53–59.
- [17] (a) G. Schlesinger, S.L. Miller, J. Mol. Evol. 19 (5) (1983) 383–390;
(b) A. Henglein, Zeitschrift Fur Naturforschung Section B-a, J. Chem. Sci. 40 (1) (1985) 100–107.
- [18] R.W.B. Pearse, A.G. Gaydon, The Identification of Molecular Spectra, 4th ed., Chapman and Hall, London, 1976.
- [19] N.M. Navarro, R. Pflieger, S.I. Nikitenko, Ultrason. Sonochem. 21 (3) (2014) 1026–1029.
- [20] (a) H.L. Wallaart, B. Piar, M.Y. Perrin, J.P. Martin, Chem. Phys. Lett. 246 (6) (1995) 587–593;
(b) W. Urban, J.X. Lin, V.V. Subramaniam, M. Havenith, J.W. Rich, Chem. Phys. 130 (1–3) (1989) 389–399.
- [21] A. Kushwaha, R.K. Thareja, Appl. Opt. 47 (31) (2008) G65–G71.